

A new tyrannosaurid (Dinosauria: Theropoda) from the Upper Cretaceous Menefee Formation of New Mexico

Andrew T. McDonald¹, Douglas G. Wolfe² and Alton C. Dooley Jr¹

¹ Western Science Center, Hemet, CA, USA

² Zuni Dinosaur Institute for Geosciences, Springerville, AZ, USA

ABSTRACT

The giant tyrannosaurids were the apex predators of western North America and Asia during the close of the Cretaceous Period. Although many tyrannosaurid species are known from numerous skeletons representing multiple growth stages, the early evolution of Tyrannosauridae remains poorly known, with the well-known species temporally restricted to the middle Campanian-latest Maastrichtian (~77–66 Ma). The recent discovery of a new tyrannosaurid, *Lythronax argestes*, from the Wahweap Formation of Utah provided new data on early Campanian (~80 Ma) tyrannosaurids. Nevertheless, the early evolution of Tyrannosauridae is still largely unsampled. We report a new tyrannosaurid represented by an associated skeleton from the lower Campanian Allison Member of the Menefee Formation of New Mexico. Despite fragmentation of much of the axial and appendicular skeleton prior to discovery, the frontals, a metacarpal, and two pedal phalanges are well-preserved. The frontals exhibit an unambiguous autapomorphy and a second potential autapomorphy that distinguish this specimen from all other tyrannosaurids. Therefore, the specimen is made the holotype of the new genus and species *Dynamoterror dynastes*. A phylogenetic analysis places *Dynamoterror dynastes* in the tyrannosaurid subclade Tyrannosaurinae. Laser-scanning the frontals and creation of a composite 3-D digital model allows the frontal region of the skull roof of *Dynamoterror* to be reconstructed.

Submitted 12 June 2018

Accepted 12 September 2018

Published 9 October 2018

Corresponding author

Andrew T. McDonald, amcdonald@westerncentermuseum.org

Academic editor

John Hutchinson

Additional Information and Declarations can be found on page 21

DOI 10.7717/peerj.5749

© Copyright

2018 McDonald et al.

Distributed under

Creative Commons CC-BY 4.0

OPEN ACCESS

Subjects Evolutionary Studies, Paleontology, Taxonomy

Keywords *Dynamoterror dynastes*, Tyrannosauridae, Allison member, Menefee formation

INTRODUCTION

During most of the Late Cretaceous Epoch, the interior of North America was inundated by a shallow epicontinental seaway, with two landmasses on either side remaining as dry land: Appalachia in the east and Laramidia in the west (Fig. 1 in [Sampson et al. \(2010\)](#)). Tyrannosauroid theropods were the largest dinosaurian predators in Appalachia, Laramidia, and Asia during the Campanian and Maastrichtian ages ([Loewen et al., 2013](#); [Brusatte & Carr, 2016](#)), approximately the final 15 million years of the Late Cretaceous before the K–Pg mass extinction ([Cohen et al., 2013](#); [Renne et al., 2013](#)). The Appalachian record is sparse, consisting of two large-bodied tyrannosauroid taxa, *Appalachiosaurus montgomeriensis* and *Dryptosaurus aquilunguis*, each known

from a single associated skeleton (Carr, Williamson & Schwimmer, 2005; Brusatte, Benson & Norell, 2011).

In contrast, the Campanian–Maastrichtian record of tyrannosauroids from Asia and especially Laramidia is extensive, consisting of numerous representatives of Tyrannosauridae, the largest and most derived tyrannosauroids. The Asian record of Tyrannosauridae includes the unusual, small-bodied, longirostrine alioramins (*Alioramus remotus* (Kurzanov, 1976), *Alioramus altai* (Brusatte et al., 2009), and *Qianzhousaurus sinensis* (Lü et al., 2014)), numerous skeletons of the immense *Tarbosaurus bataar* (Hurum & Sabath, 2003; Tsuihiji et al., 2011), and the recently named large-bodied tyrannosaurid *Zhuchengtyrannus magnus* (Hone et al., 2011).

The more bountiful record of Tyrannosauridae from Laramidia includes the poorly known, small-bodied *Nanuqsaurus hoglundi* from Alaska (Fiorillo & Tykoski, 2014), and a variety of large-bodied tyrannosaurids known from multiple specimens, such as *Albertosaurus sarcophagus* (Currie, 2003; Carr, 2010), *Gorgosaurus libratus* (Currie, 2003), and *Daspletosaurus torosus* (Russell, 1970; Currie, 2003) from Alberta; *Daspletosaurus horneri* from Montana (Carr et al., 2017); *Teratophoneus curriei* from Utah (Carr et al., 2011; Loewen et al., 2013); *Bistahieversor sealeyi* from New Mexico (Carr & Williamson, 2010), which is the sister taxon of Tyrannosauridae (Carr & Williamson, 2010; Brusatte & Carr, 2016); and the latest and most colossal of the tyrannosaurids, *Tyrannosaurus rex*, known from many locations throughout the western United States and Canada (Brochu, 2003; Currie, 2003; Carr & Williamson, 2004; Sampson & Loewen, 2005). There is also the incomplete skeleton of *Labocania anomala* from Baja California (Molnar, 1974), which is of uncertain phylogenetic affinities but might be a tyrannosauroid (Holtz, 2004).

Although exceptionally rich, the tyrannosaurid record from Laramidia is temporally restricted to between approximately 77.0 Ma (*Daspletosaurus torosus* (Currie, 2003; Carr et al., 2017; Fowler, 2017)) and 66.0 Ma (*Tyrannosaurus rex* (Carr & Williamson, 2004; Holtz, 2004)), obscuring the earlier evolution of the group. The recent discovery of a new tyrannosaurid, *Lythronax argestes*, from the Wahweap Formation of Utah (Loewen et al., 2013), provided the first extensive morphological data for an early Campanian (~80 Ma) tyrannosaurid from Laramidia. Herein we describe a new genus and species of tyrannosaurid from the lower Campanian Allison Member of the Menefee Formation in the San Juan Basin of northwestern New Mexico. The new taxon is known from an incomplete but associated skeleton including cranial and postcranial elements, and provides further insight into the morphology and diversity of tyrannosaurids from the early Campanian of Laramidia.

MATERIALS AND METHODS

The specimen described herein was collected under permit NM12-03S issued by the US Bureau of Land Management (BLM).

The electronic version of this article in portable document format will represent a published work according to the International Commission on Zoological Nomenclature (ICZN), and hence the new names contained in the electronic version are effectively

published under that Code from the electronic edition alone. This published work and the nomenclatural acts it contains have been registered in ZooBank, the online registration system for the ICZN. The ZooBank LSIDs (Life Science Identifiers) can be resolved and the associated information viewed through any standard web browser by appending the LSID to the prefix <http://zoobank.org/>. The LSID for this publication is urn:lsid:zoobank.org:pub:E6547114-4285-49BB-AF82-1280F631748F. The online version of this work is archived and available from the following digital repositories: PeerJ, PubMed Central and CLOCKSS.

Phylogenetic analysis

The data matrix of *Carr et al. (2017)* was used to test the relationships of the Allison Member tyrannosaurid; the addition of the new taxon was the only change to the matrix. The data matrix consisted of 34 taxa and 386 characters. The new taxon could be coded for only nine of the characters (S1 Codings and Measurements of UMNH VP 28348).

The matrix was analyzed in TNT 1.5 (*Goloboff & Catalano, 2016*). All 49 characters treated as ordered by *Carr et al. (2017)* were again treated as ordered. We followed the procedure of *Brusatte & Carr (2016)*. *Allosaurus* was designated as the outgroup. The matrix was first analyzed using a New Technology Search, with the default parameters for sectorial search, ratchet, tree drift, and tree fusion; a random seed of 1; 10 replicates; and the number of times to find a minimum length tree set at 10. This search examined 69,709,132 rearrangements and recovered 12 most parsimonious trees of 813 steps, consistency index of 0.552, and retention index of 0.803. These 12 trees were then examined using the tree bisection reconnection swapping algorithm, which examined 279,310 rearrangements and recovered 18 most parsimonious trees. The strict consensus of these 18 trees was then derived in TNT. Bremer support values for the strict consensus cladogram were then calculated in TNT.

RESULTS

Systematic paleontology

Dinosauria *Owen, 1842, sensu Baron, Norman & Barrett, 2017*

Theropoda *Marsh, 1881, sensu Baron, Norman & Barrett, 2017*

Coelurosauria *Huene, 1914, sensu Sereno, McAllister & Brusatte, 2005*

Tyrannosauroidae *Osborn, 1906, sensu Walker, 1964; Sereno, McAllister & Brusatte, 2005*

Tyrannosauridae *Osborn, 1906, sensu Sereno, McAllister & Brusatte, 2005*

Tyrannosaurinae *Osborn, 1906, sensu Matthew & Brown, 1922; Sereno, McAllister & Brusatte, 2005*

Dynamoterror dynastes gen. et sp. nov.

Holotype: UMNH VP 28348, incomplete associated skeleton including the left and right frontals, four fragmentary vertebral centra, fragments of dorsal ribs, right metacarpal II, supraacetabular crest of the right ilium, unidentifiable fragments of long bones, phalanx 2 of left pedal digit IV, and phalanx 4 of left pedal digit IV.

Etymology: *Dynamoterror* is derived from the transliterated Greek word *dynamis* (“power”) and the Latin word *terror*. The specific name, *dynastes*, is a Latin word meaning “ruler.” The intended meaning of the binomen is “powerful terror ruler.” The name also honors the binomen “*Dynamosaurus imperiosus*” ([Osborn, 1905](#)), a junior synonym of *Tyrannosaurus rex* ([Osborn, 1905, 1906](#)), but a particular childhood favorite of the lead author.

Locality: UMNH VP 28348 was collected in San Juan County, New Mexico, on land administered by the US BLM. Precise locality data are on file at UMNH and the BLM.

Horizon: UMNH VP 28348 was collected from outcrops of the Juans Lake Beds ([Miller, Carey & Thompson-Rizer, 1991](#)), upper part of the Allison Member, Menefee Formation; lower Campanian, Upper Cretaceous. [Lucas et al. \(2005\)](#) produced a radioisotopic date of 78.22 ± 0.26 Ma from a bentonite layer near the top of the Menefee Formation in the Gallina hogback in the eastern part of the San Juan Basin. In the part of the San Juan Basin where UMNH VP 28348 was collected, the overlying Cliff House Sandstone contains fossils of the ammonoid *Baculites perplexus* ([Siemers & King, 1974](#)), corresponding to between 78.0 and 78.5 Ma ([Molenaar et al., 2002](#)). According to the regional stratigraphic correlation chart of [Molenaar et al. \(2002\)](#), the Menefee Formation spans approximately 84.0–78.5 Ma, based upon correlations with marine biostratigraphic zones. This age range corresponds to uppermost Santonian—middle Campanian ([Cohen et al., 2013](#)).

Specific diagnosis (as for genus by monotypy): tyrannosaurine tyrannosaurid distinguished by two autapomorphies on the frontals: (1) prefrontonasal and prefrontolacrimal processes are in close proximity, separated only by a shallow notch; and (2) subrectangular, concave, laterally projecting caudal part of the postorbital suture, separated from the rostral part by a deep groove. The second autapomorphy should be treated as provisional, given the ontogenetic variation observed in this region of the frontal in other tyrannosaurids ([Carr & Williamson, 2004](#)) (see description of the lateral surface of the frontal below). In the context of the phylogenetic analysis of [Carr et al. \(2017\)](#), which is used herein, UMNH VP 28348 exhibits a feature that supports its affinities among derived tyrannosauroids (156¹, “frontal, dorsotemporal fossa, medial extension, dorsal view: meets opposing fossa at the midline”; also present in *Timurlengia euotica*, *Xionguanlong baimoensis*, *B. sealeyi*, and Tyrannosauridae), and a feature identified by [Carr et al. \(2017\)](#) as an unambiguous synapomorphy of “derived tyrannosaurines” (157¹, “frontal, sagittal crest, form, dorsal and lateral views: present and pronounced (dorsoventrally tall), single structure”).

Description

UMNH VP 28348 was collected at a single locality; as there is no duplication, morphological inconsistency, or size incompatibility among the identifiable elements, all bones collected from the site are regarded as pertaining to a single tyrannosaurid individual. All elements were collected as float in 2012. A test excavation that same year and subsequent visits in 2013 and 2018 did not reveal additional bones at the site.

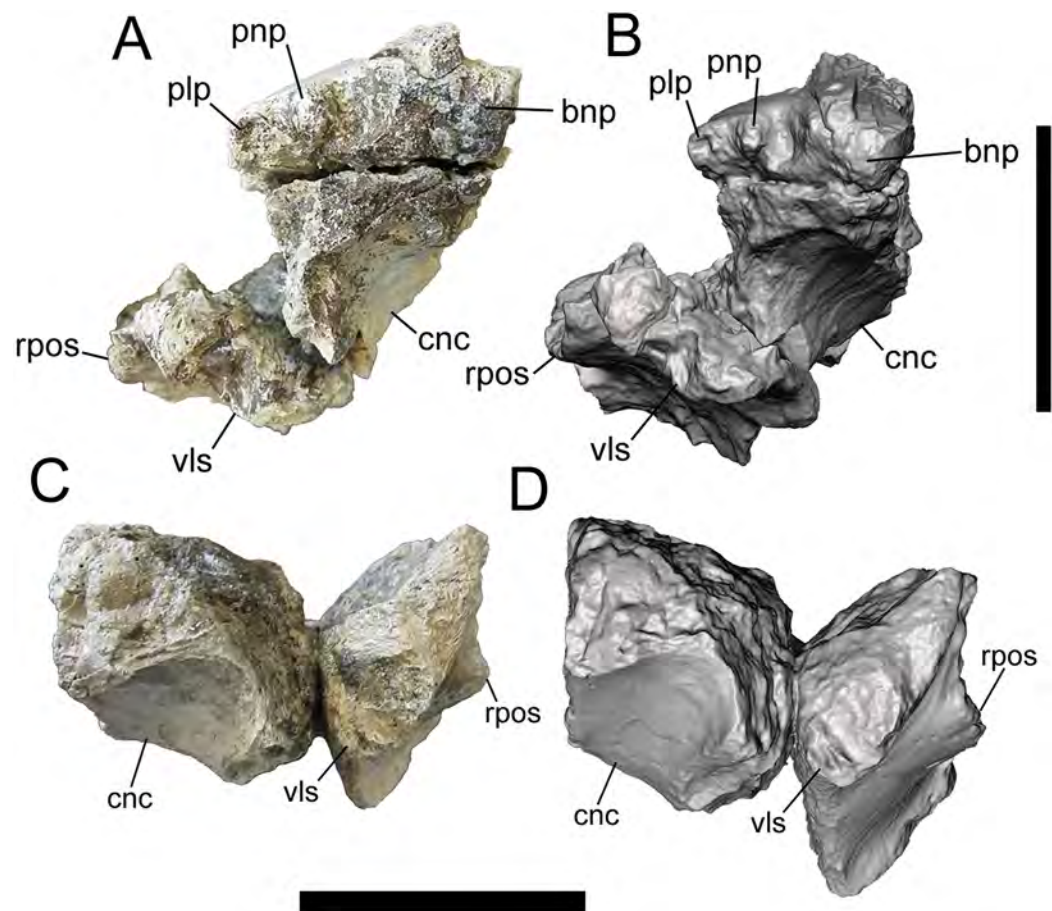


Figure 1 Frontals of UMNH VP 28348 in rostral view. Photographs and 3-D models of right (A, B) and left (C, D) frontals of UMNH VP 28348. Abbreviations: bnp, basal of nasal process; cnc, caudal extent of nasal cavity; plp, prefrontolacrimal process; pnp, prefrontonasal process; rpos, rostral part of postorbital suture; vls, ventrolateral part of lacrimal suture. Scale bars equal five cm.

Full-size DOI: [10.7717/peerj.5749/fig-1](https://doi.org/10.7717/peerj.5749/fig-1)

Measurements of select cranial and appendicular elements of UMNH VP 28348 are available in the supplementary information (S1 Codings and Measurements of UMNH VP 28348). Only those elements of UMNH VP 28348 that are identifiable based upon comparison with other tyrannosaurids are described.

Previous discoveries of tyrannosaurids in the Menefee Formation include tooth fragments and a metatarsal reported by [Hunt & Lucas \(1993\)](#), and another tooth fragment reported by [Lewis \(2006\)](#). Lack of overlapping material precludes referral of any of these elements to *Dynamoterror dynastes*. UMNH VP 28348 is the first associated tyrannosaurid skeleton reported from the Menefee Formation.

Frontals

The right and left frontals both are incomplete; however, between them, they exhibit nearly the entire frontal morphology, with the exception of the rostral end of the nasal process (Figs. 1–7). Many fine details are preserved, allowing thorough comparisons with other tyrannosaurid frontals. Unfortunately, no frontals are known for the Late Cretaceous

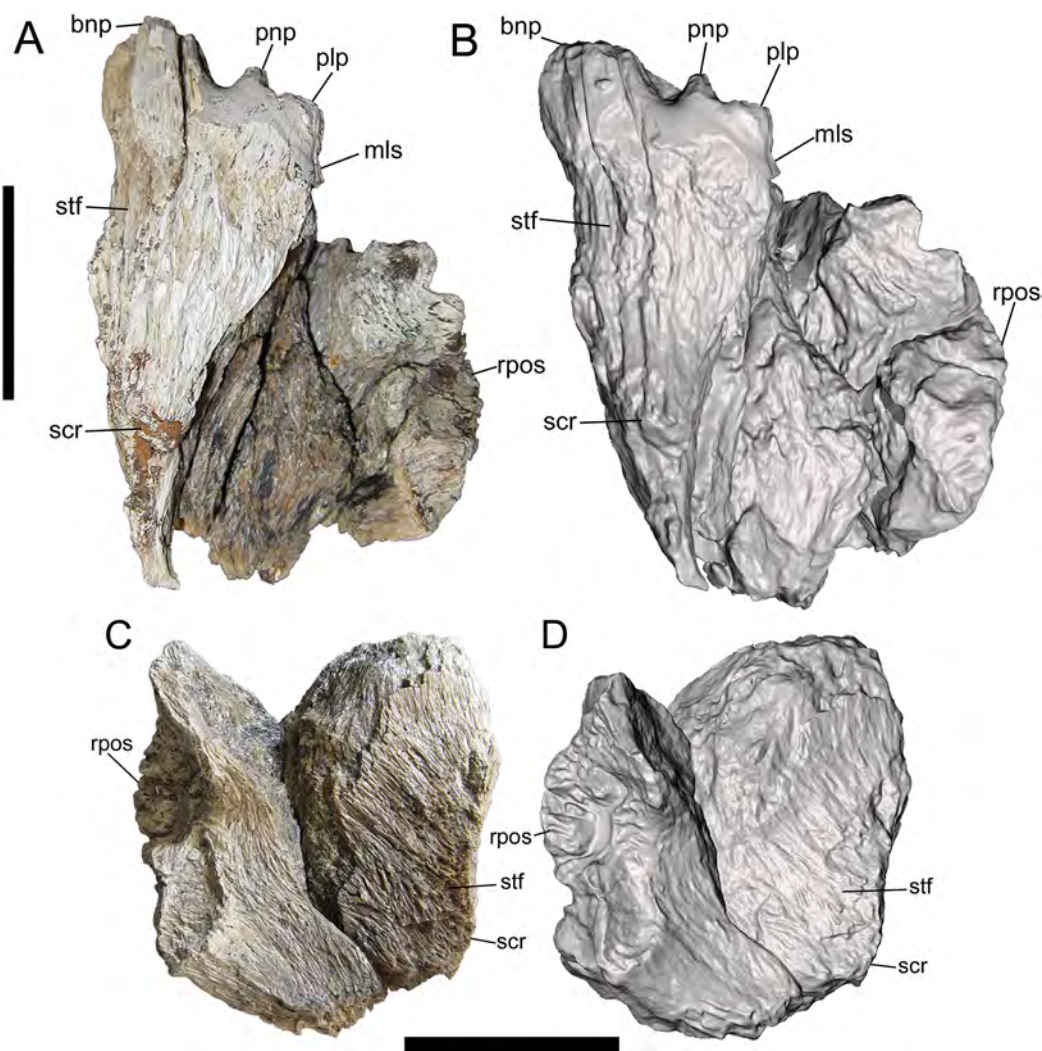


Figure 2 Frontals of UMNH VP 28348 in dorsal view. Photographs and 3-D models of right (A, B) and left (C, D) frontals of UMNH VP 28348. Abbreviations: bnp, basal of nasal process; mls, medial-most point of lacrimal suture; plp, prefrontolacrimal process; pnp, prefrontonasal process; rpos, rostral part of postorbital suture; scr, sagittal crest; stf, supratemporal fossa. Scale bars equal five cm.

Full-size DOI: 10.7717/peerj.5749/fig-2

Appalachian outgroups of Tyrannosauridae, *Appalachiosaurus montgomeriensis* and *Dryptosaurus aquilunguis* (Carr, Williamson & Schwimmer, 2005; Brusatte, Benson & Norell, 2011). However, comparisons were possible with *B. sealeyi* (Lehman & Carpenter, 1990; Carr & Williamson, 2000, 2010), which is the closest outgroup of Tyrannosauridae (Carr & Williamson, 2010; Brusatte & Carr, 2016), and with numerous members of Tyrannosauridae, including the albertosaurines *Albertosaurus sarcophagus* and *G. libratus* (Currie, 2003) and the tyrannosaurines *Alioramus altai* (Bever et al., 2013), *Daspletosaurus* sp. (Currie, 2003), *L. argestes* (UMNH VP 20200) (Loewen et al., 2013), *Teratophoneus curriei* (BYU 8120/9396, UMNH VP 16690) (Carr et al., 2011; Loewen et al., 2013), *N. hoglundi* (Fiorillo & Tykoski, 2014), *Tarbosaurus bataar* (Hurum & Sabath, 2003),

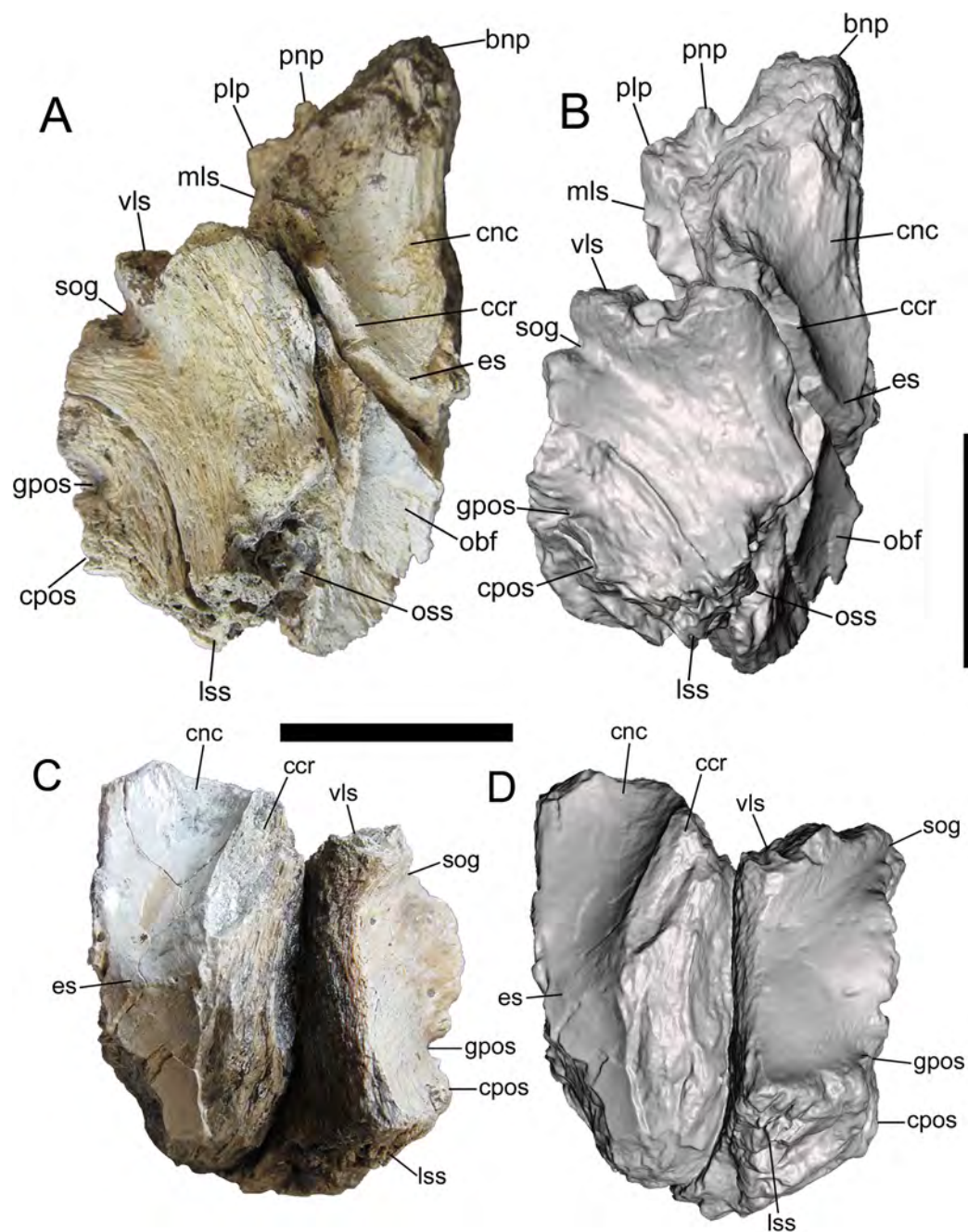


Figure 3 Frontals of UMNH VP 28348 in ventral view. Photographs and 3-D models of right (A, B) and left (C, D) frontals of UMNH VP 28348. Abbreviations: bnp, basal of nasal process; ccr, crista cranii; cnc, caudal extent of nasal cavity; cpos, caudal part of postorbital suture; es, ethmoid scar; gpos, groove between rostral and caudal parts of postorbital suture; lss, laterosphenoid suture; mls, medial-most point of lacrimal suture; obf, olfactory bulb fossa; oss, orbitosphenoid suture; plp, prefrontolacrimal process; pnp, prefrontonasal process; sog, supraorbital groove; vls, ventrolateral part of lacrimal suture. Scale bars equal five cm. [Full-size !\[\]\(fd7fe780e8fd8eece60268c87d0c3e04_img.jpg\) DOI: 10.7717/peerj.5749/fig-3](https://doi.org/10.7717/peerj.5749/fig-3)

Tyrannosaurus rex (LACM 23845, LACM 150167) (*Osborn, 1912; Brochu, 2003; Carr & Williamson, 2004; Larson, 2008*), and an unnamed tyrannosaurine from the Aguja Formation of Texas (*Lehman & Wick, 2012*).

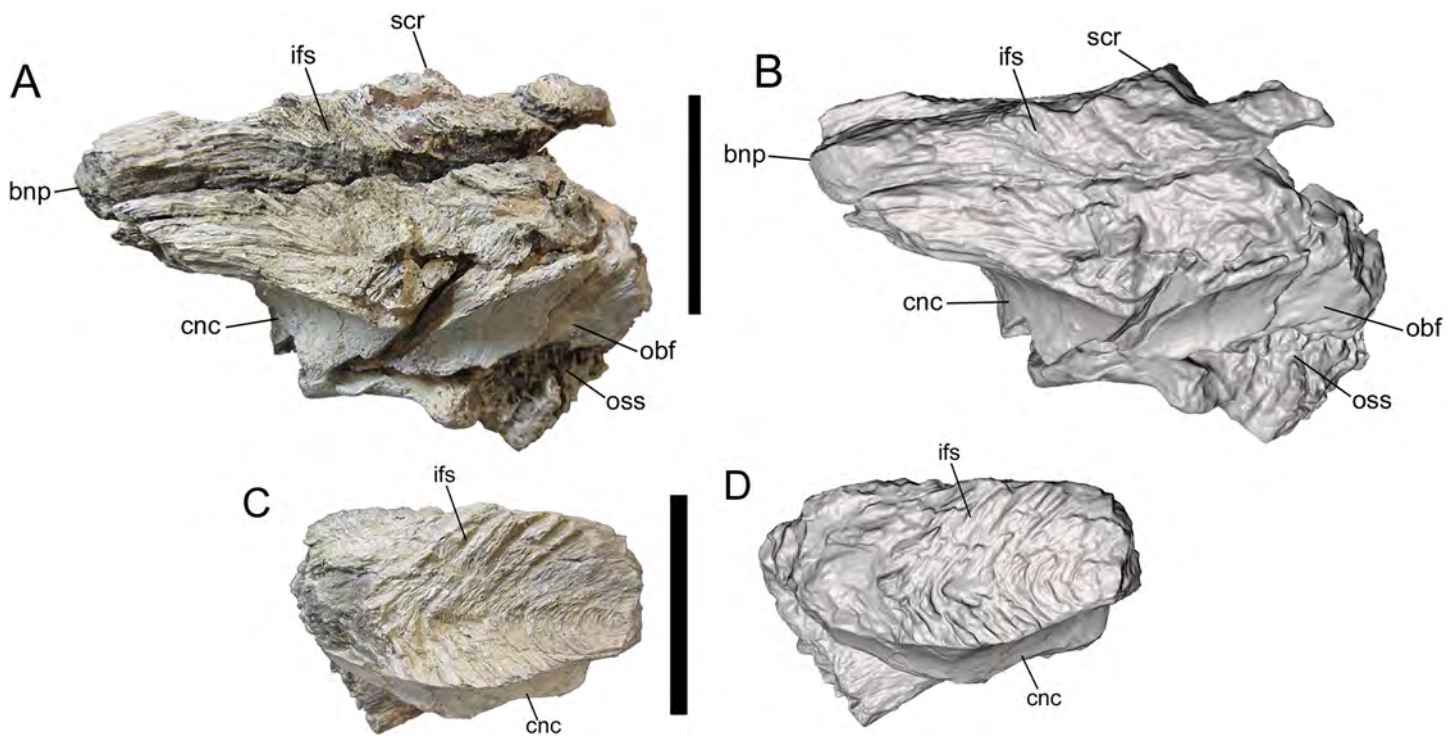


Figure 4 Frontals of UMNH VP 28348 in medial view. Photographs and 3-D models of right (A, B) and left (C, D) frontals of UMNH VP 28348. Abbreviations: bnp, basal of nasal process; cnc, caudal extent of nasal cavity; ifs, interfrontal suture; obf, olfactory bulb fossa; oss, orbitosphenoid suture; scr, sagittal crest. Scale bars equal five cm. [Full-size !\[\]\(5fd6ef84f97f42d7f8b34275f1b65312_img.jpg\) DOI: 10.7717/peerj.5749/fig-4](https://doi.org/10.7717/peerj.5749/fig-4)

The length, width, and depth of the frontals of UMNH VP 28348 were measured after the methodology of [Currie \(2003\)](#). The overall dimensions of the right frontal of UMNH VP 28348 are similar to those of LACM 23845 (Table 2 in [Currie \(2003\)](#)), a subadult specimen of *Tyrannosaurus rex* ([Molnar, 1980](#); [Carr & Williamson, 2004](#)) (S1 Codings and Measurements of UMNH VP 28348). Although complete length cannot be measured for the frontals of UMNH VP 28348 due to breakage of the nasal processes, width and depth can be measured for the right frontal. The ratio of depth to width for the right frontal is 0.57, comparable to frontals of subadult and adult *Daspletosaurus* sp. (0.50–0.66) and *Tyrannosaurus rex* (0.59–0.67, including LACM 23845 (0.62)), calculated from the measurements provided by [Currie \(2003](#); Table 2). In tyrannosaurids, the depth of the frontal exhibits positive allometry relative to width during the course of ontogeny ([Currie, 2003](#)). Coupled with the measurements and depth/width ratio, this suggests that UMNH VP 28348 represents a subadult or adult individual.

The frontals are described together as a single unit, though it is noted whether a feature is most clearly preserved on the right, left, or both frontals. Given the complexity of the morphology of the frontals, the description is divided into six sections, detailing the rostral, dorsal, ventral, medial, lateral, and caudal surfaces.

Rostral surface

The medial-most feature on the rostral surface is the base of the nasal process. The nasal process projects rostrally, but is missing its rostral end (right frontal)

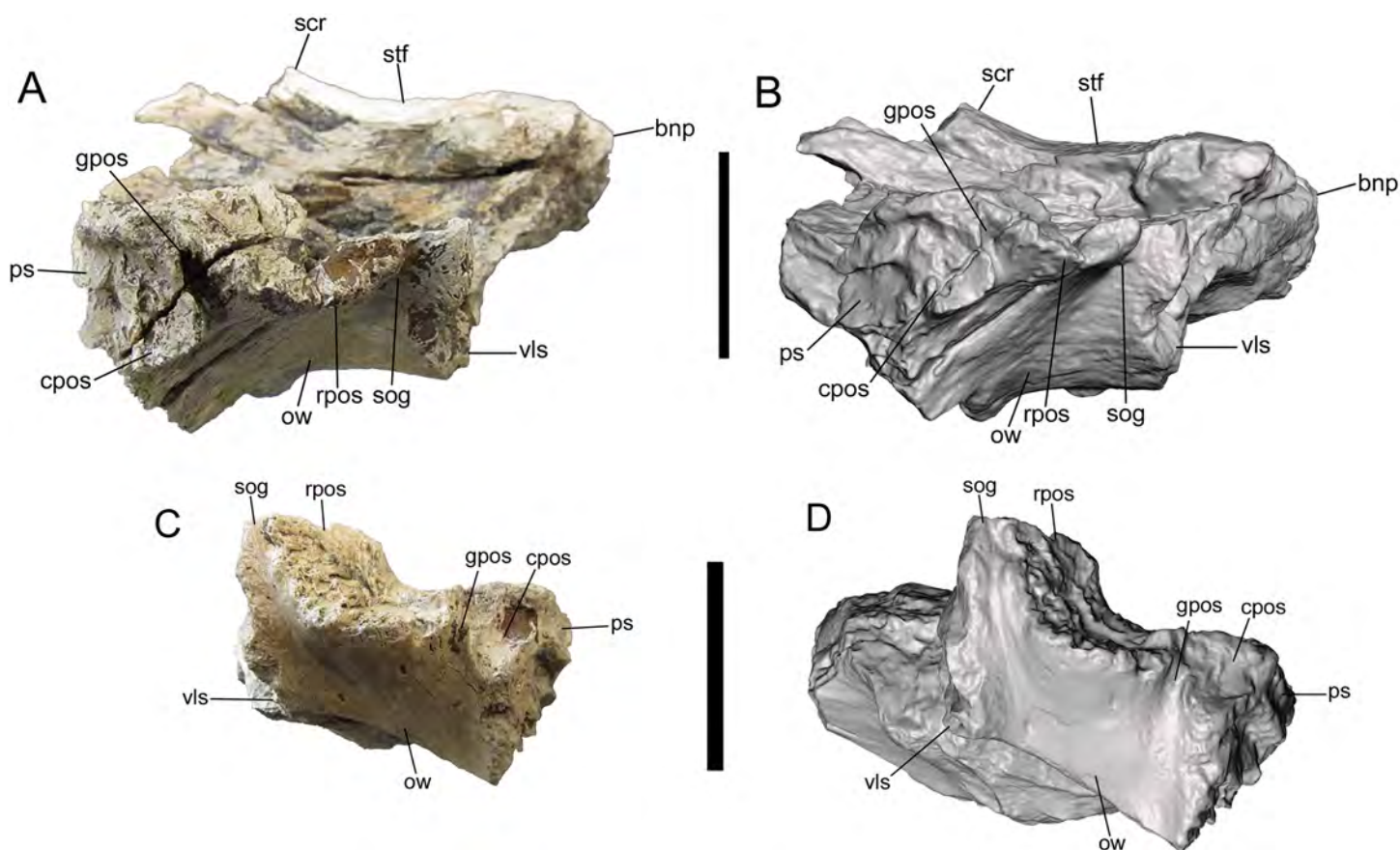


Figure 5 Frontals of UMNH VP 28348 in lateral view. Photographs and 3-D models of right (A, B) and left (C, D) frontals of UMNH VP 28348. Abbreviations: bnp, basal of nasal process; cpos, caudal part of postorbital suture; gpos, groove between rostral and caudal parts of postorbital suture; ow, orbital wall; ps, parietal suture; rpos, rostral part of postorbital suture; scr, sagittal crest; sog, supraorbital groove; stf, supratemporal fossa; vls, ventrolateral part of lacrimal suture. Scale bars equal five cm. [Full-size !\[\]\(43e4e85f3e07c993849f98a1fa87e486_img.jpg\) DOI: 10.7717/peerj.5749/fig-5](https://doi.org/10.7717/peerj.5749/fig-5)

(Figs. 1A, 1B, 2A and 2B). Lateral to the base of the nasal process is a deep notch that marks the caudal-most point of the contact with the nasal (right frontal). Lateral to this deep notch is the small, conical, rostrally projecting prefrontonasal process (right frontal) (Figs. 1A, 1B, 2A and 2B), as in *Teratophoneus curriei* (BYU 8120/9396) and *L. argestes* (UMNH VP 20200) (Fig. 2E in [Loewen et al. \(2013\)](#)). Lateral to the prefrontonasal process is another, shallower notch, which marks the location of prefrontal exposure on the skull roof. Lateral to this notch is a circular broken surface that represents the base of another small conical process similar to the prefrontonasal process (right frontal) (Figs. 1A, 1B, 2A and 2B). This more laterally situated small conical process is the prefrontolacrimal process. This small prefrontolacrimal process differs from the much larger, rostrocaudally long prefrontolacrimal processes that separate the prefrontal and lacrimal sutures in *Teratophoneus curriei* (BYU 8120/9396) (Fig. 3E in [Loewen et al. \(2013\)](#)) and *N. hoglundi* (Figs. 3F–3I in [Fiorillo & Tykoski \(2014\)](#)). It is similar to the rostrocaudally short prefrontolacrimal processes of *L. argestes* (UMNH VP 20200) (Fig. 2E in [Loewen et al. \(2013\)](#)), *Daspletosaurus* sp. (Figs. 20A, 20C in [Currie \(2003\)](#)), *Tyrannosaurus rex* (LACM 23845, LACM 150167) ([Larson, 2008](#)), and

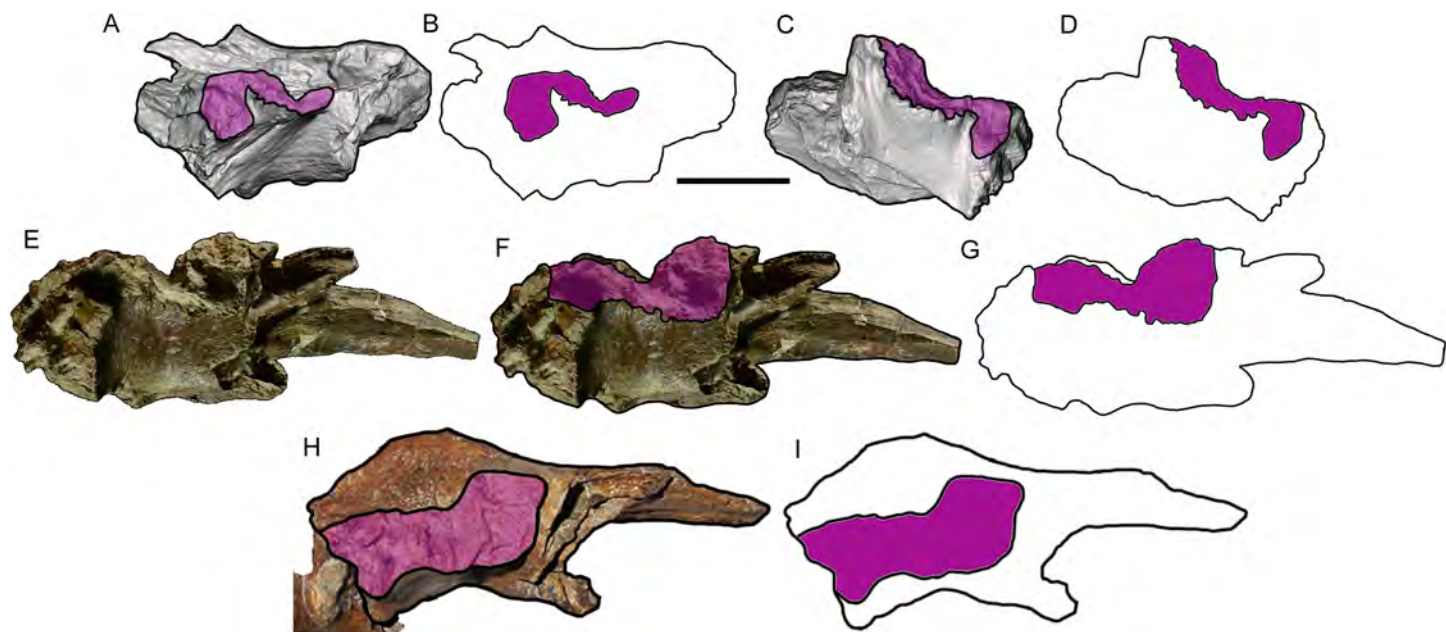


Figure 6 Comparison among derived tyrannosaurine frontals. Digital models and line drawings of the right (A, B) and left (C, D) frontals of *Dynamoterror dynastes*, UMNH VP 28348, in lateral view. The postorbital suture is highlighted in purple. Scale bar equals five cm for A–D. BYU 8120/9396, right frontal of *Teratophoneus curriei* in lateral view, shown as a photograph (E), photograph with the postorbital suture highlighted in purple (F), and a line drawing with the postorbital suture highlighted in purple (G). Photograph of BYU 8120/9396 courtesy of Rod Scheetz (BYU) and is used here with permission. Additional anatomical information from UMNH VP 16690 (Fig. 3E in [Loewen et al. \(2013\)](#)). UMNH VP 20200, right frontal of *Lythronax argestes* in lateral view, shown as an image with the postorbital suture highlighted in purple (H) (modified from Fig. 2E in [Loewen et al. \(2013\)](#)), and a line drawing with the postorbital suture highlighted in purple (I). [Full-size](#) DOI: 10.7717/peerj.5749/fig-6

Tarbosaurus bataar (Figs. 8, 17 in [Hurum & Sabath \(2003\)](#)). The close proximity of the prefrontonasal and prefrontolacrimal processes, which are separated only by a narrow notch, is unique to UMNH VP 28348 and is an autapomorphy of *Dynamoterror dynastes*.

Lateral to the prefrontolacrimal process is a smooth surface that extends caudally and then begins to curve laterally, where it is truncated by a broken surface (right frontal) (Figs. 2A and 2B). This surface marks the medial-most point of the lacrimal suture. Lateral to this surface, the right frontal is missing much of the lacrimal suture. However, the ventrolateral portion of the lacrimal suture is preserved on the right frontal (Figs. 1A and 2B), and to a lesser extent on the left frontal (Figs. 1C and 1D). This part of the suture forms a dorsoventrally deep, rostrally facing cup-like structure that is rostrally concave and ventrolaterally convex, as in *L. argestes* (UMNH VP 20200) (Figs. 2E, 5 in [Loewen et al. \(2013\)](#)), *Teratophoneus curriei* (BYU 8120/9396) (Fig. 3E in [Loewen et al. \(2013\)](#)), *Daspletosaurus* sp. (Fig. 20 in [Currie \(2003\)](#)), *Tyrannosaurus rex* (LACM 150167) ([Larson, 2008](#)), *Tarbosaurus bataar* (Figs. 8, 17 in [Hurum & Sabath \(2003\)](#)), and *N. hoglundii* (Figs. 3F–I, 4 in [Fiorillo & Tykoski \(2014\)](#)). In the Aguja tyrannosaurine, the lacrimal contact is a deep, rostroventrally directed recess (Figs. 3, 4 in [Lehman & Wick \(2012\)](#)).

Dorsal surface

Only the rostromedial region of the dorsal surface is preserved on the right frontal (Figs. 2A and 2B). The left frontal preserves much of the dorsal surface, though weathering

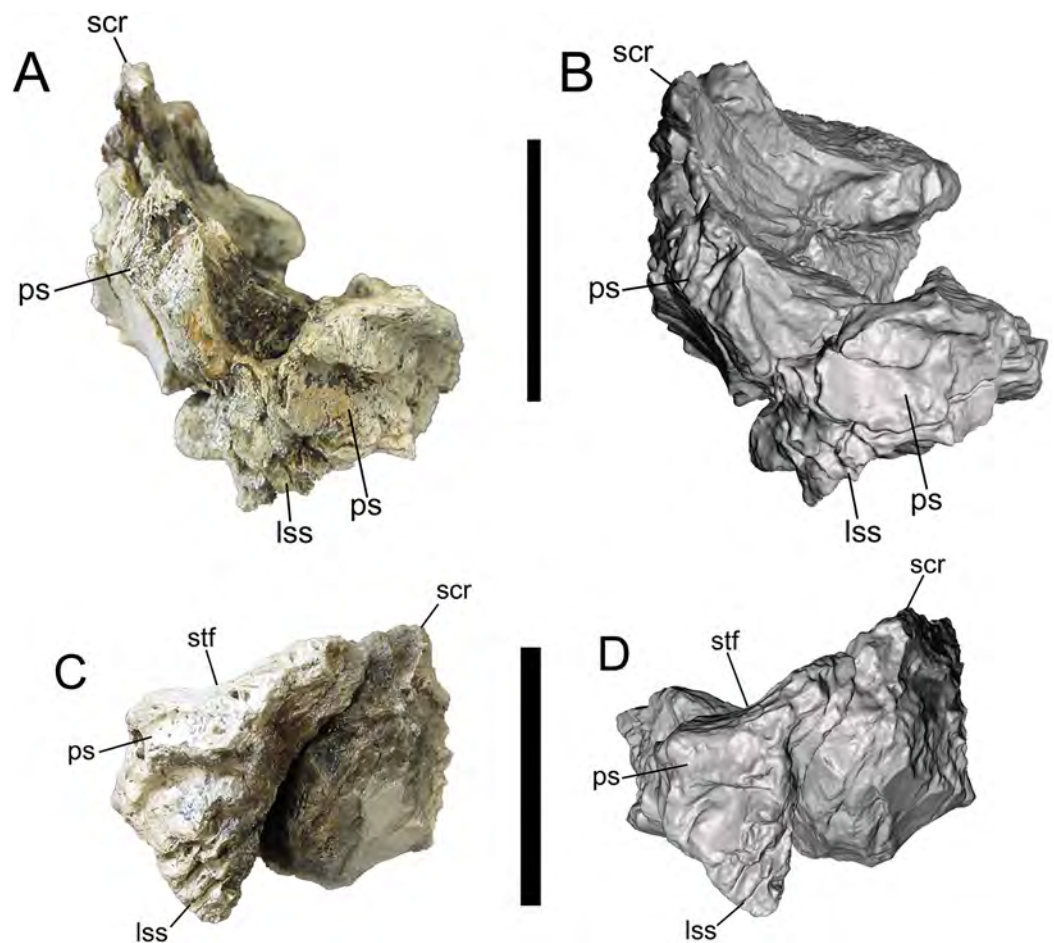


Figure 7 Frontals of UMNH VP 28348 in caudal view. Photographs and 3-D models of right (A, B) and left (C, D) frontals of UMNH VP 28348. Abbreviations: lss, laterosphenoid suture; ps, parietal suture; scr, sagittal crest; stf, supratemporal fossa. Scale bars equal five cm.

Full-size  DOI: [10.7717/peerj.5749/fig-7](https://doi.org/10.7717/peerj.5749/fig-7)

has stripped it of the outermost layer of cortical bone (Figs. 2C and 2D). However, as shown by preserved patches of complete bone surface near the lateral margin, only a fraction of a millimeter of thickness is missing from the dorsal surface of the left frontal.

On the dorsal surface of the right frontal, there is a slight swelling immediately caudal to the nasal, prefrontonasal, and prefrontolacrimal processes (Figs. 2A and 2B). Caudal to this swelling, the dorsal surface of the right frontal becomes gently concave and begins to slope caudolaterally to form the frontal portion of the supratemporal fossa (Figs. 2A and 2B). The rest of the frontal portion of the supratemporal fossa is preserved on the left frontal, on which the dorsal surface slopes caudolaterally toward the parietal suture where it formed a contiguous supratemporal fossa with the dorsolateral surface of the parietal (Figs. 2C and 2D).

On both frontals, the dorsal surface rises caudomedially to form the frontal portion of the sagittal crest (Fig. 2). The sagittal crest is better preserved on the right frontal. Although broken caudally, the height of the preserved portion above the supratemporal fossa and the curvature of the bone grain indicates that the crest would have continued

to rise beyond the damaged surface and been very tall. A prominent sagittal crest that extends far onto the frontals is also present in the tyrannosaurines *Daspletosaurus* sp. (Fig. 20B in [Currie \(2003\)](#)), *Tyrannosaurus rex* (LACM 23845, LACM 150167) (Fig. 20 in [Brochu \(2003\)](#)) ([Carr & Williamson, 2004](#); [Larson, 2008](#)), *Teratophoneus curriei* (BYU 8120/9396) (Fig. 3E in [Loewen et al. \(2013\)](#)), *L. argestes* (UMNH VP 20200) (Fig. 2E in [Loewen et al. \(2013\)](#)), *N. hoglundi* (Fig. 4 in [Fiorillo & Tykoski \(2014\)](#)), *Tarbosaurus bataar* (Fig. 17 in [Hurum & Sabath \(2003\)](#)), and the Aguja tyrannosaurine (Figs. 3, 4 in [Lehman & Wick \(2012\)](#)), as well as *B. sealeyi* (Fig. 2 in [Lehman & Carpenter \(1990\)](#); Fig. 1A in [Carr & Williamson \(2010\)](#)). This morphology differs from the albertosaurines *Albertosaurus sarcophagus* and *G. libratus*, which have much lower sagittal crests on the frontals ([Currie, 2003](#)). The morphology of the sagittal crest suggests that UMNH VP 28348 represents a tyrannosaurine.

Ventral surface

The detailed description of the frontals of *Alioramus altai* (see Fig. 9 in [Bever et al. \(2013\)](#)) was useful for interpreting the ventral surfaces of the frontals of UMNH VP 28348. Details of the rostral region of the ventral surface are well preserved on both frontals. This region is dominated by a rostrocaudally elongate, mediolaterally wide fossa that is defined rostrally by the prefrontal suture, medially by the interfrontal suture, laterally by the crista cranii, and caudally by the ethmoid scar ([Fig. 3](#)). When the frontals are placed in articulation, the right and left fossae form the caudal extent of the olfactory region of the nasal cavity, which was lined with mucous membrane when the animal was alive ([Witmer & Ridgely, 2009](#); [Bever et al., 2013](#)). Lateral to the fossa is the crista cranii, a thick, sharply defined ridge that extends rostromedially to caudomedially, delineating the ventral and lateral surfaces of the frontal ([Fig. 3](#)).

The rostral fossa is separated from the olfactory bulb fossa by the ethmoid scar, a subtle mediolaterally oriented ridge that branches off of the crista cranii ([Fig. 3](#)). Only a small portion of the olfactory bulb fossa is preserved on the left frontal, while the entire fossa and the surrounding features of the caudal region of the ventral surface are intact on the right frontal. The large olfactory bulb fossa is defined rostrally by the ethmoid scar, medially by the interfrontal suture, laterally by the crista cranii and orbitosphenoid suture, and caudally by the parietal suture ([Figs. 3A and 3B](#)). The orbitosphenoid suture is a subcircular, ventromedially facing concavity lined with a complex set of delicate ridges, bumps, and depressions. The orbitosphenoid suture widens caudally where it merges with the laterosphenoid suture on the caudoventral surface of the frontal.

Medial surface

The medial surface is occupied entirely by the flat, vertical interfrontal suture ([Fig. 4](#)). The suture itself is better preserved on the left frontal, and consists of a series of overlapping fine, V-shaped ridges with the V's opening rostrally.

Lateral surface

The details of the lateral surface are well-preserved on both frontals and include a number of characters of diagnostic and comparative value. The lacrimal and postorbital sutures

are separated by a narrow, deep, vertical groove (“supraorbital groove” of *Loewen et al. (2013)*) (Fig. 5). Similar supraorbital grooves are observable in *L. argestes* (UMNH VP 20200) (Fig. 2E in *Loewen et al. (2013)*), *Teratophoneus curriei* (BYU 8120/9396) (Fig. 3E in *Loewen et al. (2013)*), *Tyrannosaurus rex* (LACM 150167), *N. hoglundi* (Fig. 3F–I in *Fiorillo & Tykoski (2014)*), *Tarbosaurus bataar* (Fig. 8A, B in *Hurum & Sabath (2003)*), *B. sealeyi* (Fig. 2 “cleft in frontal” in *Lehman & Carpenter (1990)*), and the albertosaurine *Albertosaurus sarcophagus* (Fig. 7 in *Currie (2003)*). The supraorbital groove grades into the orbital wall ventrally.

The postorbital suture is divided into a large rostral part and a smaller caudal part. The ventral margin of the rostral part is convex and projects farther laterally than the dorsal margin, forming a deeply concave sutural surface (Figs. 2 and 5). The rostradorsal region of the rostral part projects dorsally, such that the rostradorsal margin is elevated far above the caudodorsal margin and the caudodorsal margin is deeply concave (Figs. 5C and 5D). Ventral to the rostral part of the postorbital suture is the deep orbital wall, which is entirely visible in lateral view (Fig. 5).

The rostral and caudal parts of the postorbital suture are separated by a deep, smooth, caudally inclined groove that opens ventrally onto the orbital wall and is roofed dorsally by the dorsal surface of the frontal. The groove is present on both frontals but is better preserved on the right (Fig. 5). While this groove might be homologous to the open foramen that penetrates the dorsal skull roof in *Tyrannosaurus rex* (Fig. 3 in *Brochu (2003)*) and/or the neurovascular foramen identified in the Aguja tyrannosaurine (Figs. 3, 4 in *Lehman & Wick (2012)*), these possibilities must await testing by the discovery of further material.

The caudal part of the postorbital suture is a subrectangular, slightly concave structure that is delineated rostrally by a rostrolaterally projecting rim that separates it from the aforementioned deep groove, ventrally by a ventrolaterally projecting rim that separates it from the orbital wall, dorsally by a laterally projecting rim that separates it from the dorsal surface of the frontal, and caudally by a more subtle and irregular rim that also marks the lateral-most point of the parietal suture (Fig. 5). This subrectangular, concave, laterally projecting caudal part appears to be unique to UMNH VP 28348 and is proposed as an autapomorphy of *Dynamoterror dynastes*, differing from the continuous rostral and caudal parts of the postorbital suture in *B. sealeyi* (Fig. 2 in *Lehman & Carpenter (1990)*; Fig. 4 in *Lehman & Wick (2012)*); the albertosaurines *Albertosaurus sarcophagus* and *G. libratus* (*Currie, 2003*); and the tyrannosaurines *Tyrannosaurus rex* (LACM 150167) (Fig. 7 in *Osborn (1912)*) (*Larson, 2008*), *L. argestes* (UMNH VP 20200) (Fig. 2E in *Loewen et al. (2013)*), *Teratophoneus curriei* (BYU 8120/9396, UMNH VP 16690) (Fig. 3E in *Loewen et al. (2013)*), *Daspletosaurus* sp. (*Currie, 2003*), *Tarbosaurus bataar* (Fig. 17C, D in *Hurum & Sabath (2003)*), and the Aguja tyrannosaurine (Figs. 3, 4 in *Lehman & Wick (2012)*). However, it should be noted that the region of the postorbital suture is subject to ontogenetic variation, particularly in changing from an area of grooves and ridges to a peg-in-socket morphology (*Carr & Williamson, 2004*). UMNH VP 28348 exhibits the latter morphology. This region of the frontal is damaged in the only known specimen of



Figure 8 Middle caudal centrum of UMNH VP 28348. Incomplete middle caudal centrum in left lateral view. Abbreviations: chf, chevron facet. Scale bar equals five cm.

Full-size  DOI: [10.7717/peerj.5749/fig-8](https://doi.org/10.7717/peerj.5749/fig-8)

N. hoglundi (Figs. 3, 4 in [Fiorillo & Tykoski \(2014\)](#)). Overall, the frontals of UMNH VP 28348 are similar to those of other tyrannosaurines, such as *Teratophoneus curriei* and *L. argestes*, but differ in the aforementioned potentially autapomorphic morphology of the caudal part of the postorbital suture ([Fig. 6](#)), though this feature should be regarded with caution.

Caudal surface

The caudal surface is occupied by two major features, the laterosphenoid and parietal sutures, which are preserved on both frontals. The laterosphenoid suture faces caudoventrally, and is ventral to the parietal suture and caudolateral to the orbitosphenoid suture ([Fig. 7](#)). The parietal suture begins caudomedial to the caudal part of the postorbital suture and extends caudomedially before curving rostromedially and dorsally toward the base of the sagittal crest.

Middle caudal centrum

Of the four fragments of vertebral centra preserved in UMNH VP 28348, only one can be placed in the vertebral column with any precision. This fragment was identified as part of the centrum of a middle caudal vertebra. As on the middle caudal centra of *Tyrannosaurus rex* (Figs. 60K–Q in [Brochu \(2003\)](#)), that of UMNH VP 28348 exhibits a pronounced, caudoventrally directed chevron articulation facet that is offset from the ventral margin of the caudal face of the centrum ([Fig. 8](#)).

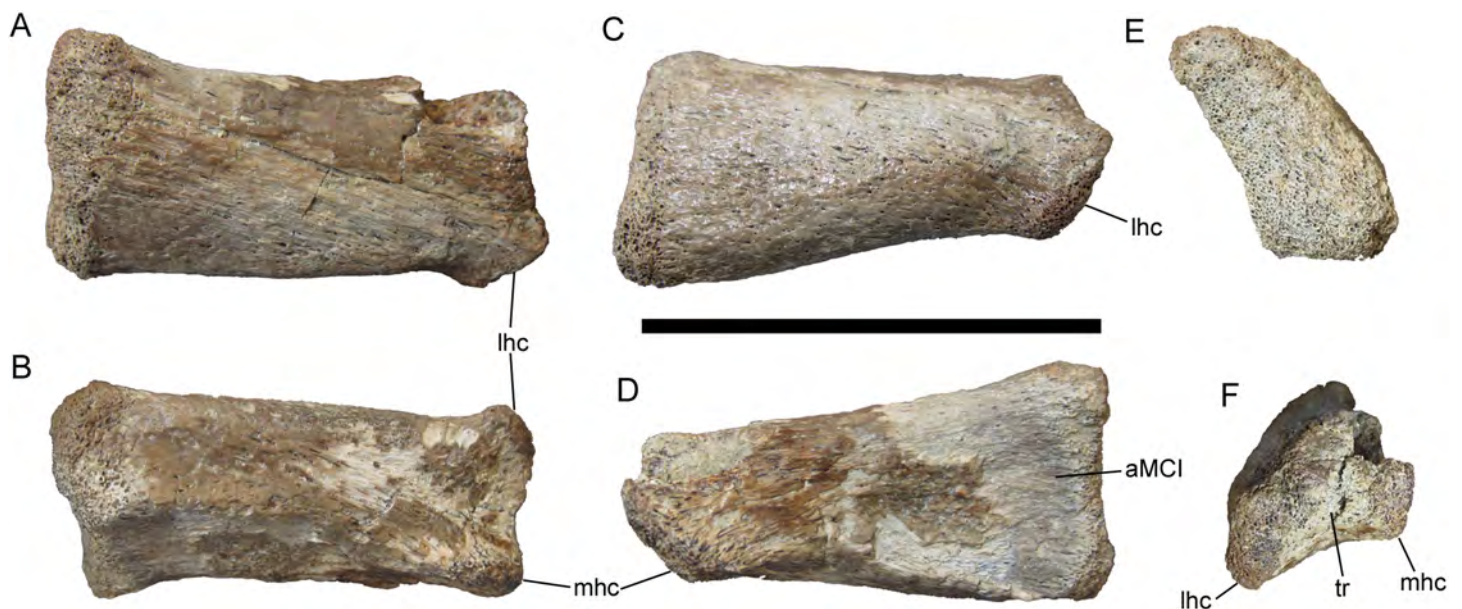


Figure 9 Right metacarpal II of UMNH VP 28348. Right metacarpal II in (A) dorsal; (B) ventral; (C) lateral; (D) medial; (E) proximal; and (F) distal views. Abbreviations: aMCI, surface for articulation with metacarpal I; lhc, lateral hemicondyle; mhc, medial hemicondyle; tr, trochlea. Scale bar equals five cm. [Full-size !\[\]\(ebfe6d37ad86655679811e032f633da4_img.jpg\) DOI: 10.7717/peerj.5749/fig-9](https://doi.org/10.7717/peerj.5749/fig-9)

Right metacarpal II

Right metacarpal II was identified based upon comparisons with the nearly complete, articulated right manus of *Tyrannosaurus rex* (Figs. 88A–D, 89 in [Brochu \(2003\)](#)) and left manus of *Daspletosaurus torosus* (Plates III, IV in [Russell \(1970\)](#)). MC II is overall nearly straight, with only a slight medial curvature toward the distal end in dorsal and ventral views (Figs. 9A and 9B). The proximal articular surface is slightly concave in lateral and medial views (Figs. 9C and 9D). In proximal view, the proximal articular surface tapers and curves medially toward its dorsal margin (Fig. 9E). The ventral surface of the shaft of MC II is flat and widens toward the distal articular surface (Fig. 9B). The dorsal and lateral surfaces of MC II are indistinct and form a gently convex surface (Figs. 9A and 9C). No articulation surface for MCIII is apparent on the lateral surface, unlike *Tyrannosaurus rex*, which exhibits a pronounced sulcus on the lateral surface of MCII near the proximal end ([Brochu, 2003](#)). The medial surface of MC II is broad and gently concave, forming a surface for articulation with the lateral surface of MC I (Fig. 9D). The distal articular surface is composed of lateral and medial hemicondyles separated by a shallow trochlea (Fig. 9F). The medial hemicondyle is missing approximately its dorsal half, making its size relative to the lateral hemicondyle impossible to judge. The lateral hemicondyle extends 0.3 cm farther distally than the medial hemicondyle (Figs. 9A–9D), as in *Tyrannosaurus rex* ([Brochu, 2003](#)).

Supraacetabular crest of right ilium

A broadly arched bone fragment was identified as the supraacetabular crest of the right ilium, based upon comparisons with ilia of *Teratophoneus curriei* (UMNH VP 16690) and *Tyrannosaurus rex* (Fig. 92 in [Brochu \(2003\)](#)). The ventral surface of this fragment is

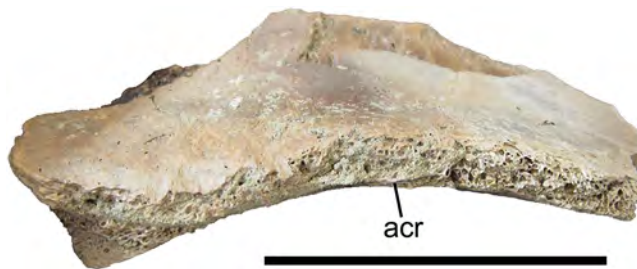


Figure 10 Supraacetabular crest of the right ilium of UMNH VP 28348. Supraacetabular crest of the right ilium in lateral view. Abbreviations: acr, rim of the acetabulum. Scale bar equals five cm.

Full-size  DOI: [10.7717/peerj.5749/fig-10](https://doi.org/10.7717/peerj.5749/fig-10)

smooth and gently concave to form the dorsal margin of the acetabulum. The lateral margin of the supraacetabular crest is very thin for most of its preserved length (0.7 cm thick at the midpoint of the preserved portion). However, the lateral margin becomes considerably thicker caudally (2.1 cm thick at its maximum preserved thickness), toward the base of the ischial peduncle (Fig. 10), as on the other tyrannosaurid ilia referenced above. The supraacetabular crest also becomes markedly thicker medially (2.5 cm thick at its maximum preserved thickness), as its dorsal margin slopes steeply dorsally to merge with the lateral surface of the blade of the ilium.

Phalanx 2 of left pedal digit IV

Two well-preserved phalanges were identified as phalanges 2 and 4 of left pedal digit IV based upon comparisons with LACM 23844, an articulated left pes of *Tyrannosaurus rex*, and the *Tyrannosaurus rex* pes described by Brochu (2003). IV-2 is missing the dorsal half of the proximal articular surface and the medial condyle (Figs. 11A–11F). The preserved portion of the proximal articular surface is subrectangular and divided into two facets by a broad, subtle ridge; the lateral facet is mediolaterally wider than the medial facet (Figs. 11A and 11C). Distal to the proximal articular surface, the shaft of IV-2 is constricted mediolaterally and dorsoventrally. On the medial surface of the shaft, immediately distal to the proximal articular surface, there is a deep circular pit with a pronounced bump ventral to it (Fig. 11E). The corresponding region on the lateral surface of the shaft is smooth and featureless (Fig. 11F). The lateral condyle is hemispherical and bears a deep fovea on its lateral surface (Fig. 11F).

Phalanx 4 of left pedal digit IV

IV-4 is much smaller than IV-2 in all dimensions (Figs. 11G–11L). As on IV-2, the proximal articular surface of IV-4 is divided into two facets; however, unlike those of IV-2, the facets of IV-4 are equal in size and demarcated by a distinct ridge (Fig. 11G). On the distal articular surface of IV-4, the medial and lateral condyles are separated by a much deeper trochlea than on IV-2 (Figs. 11H–11J). The lateral condyle is dorsoventrally deeper than the medial condyle. The medial and lateral condyles each bear a deep circular fovea, though the fovea on the lateral condyle is deeper than that on the medial (Figs. 11K and 11L), as in IV-4 of LACM 23844.

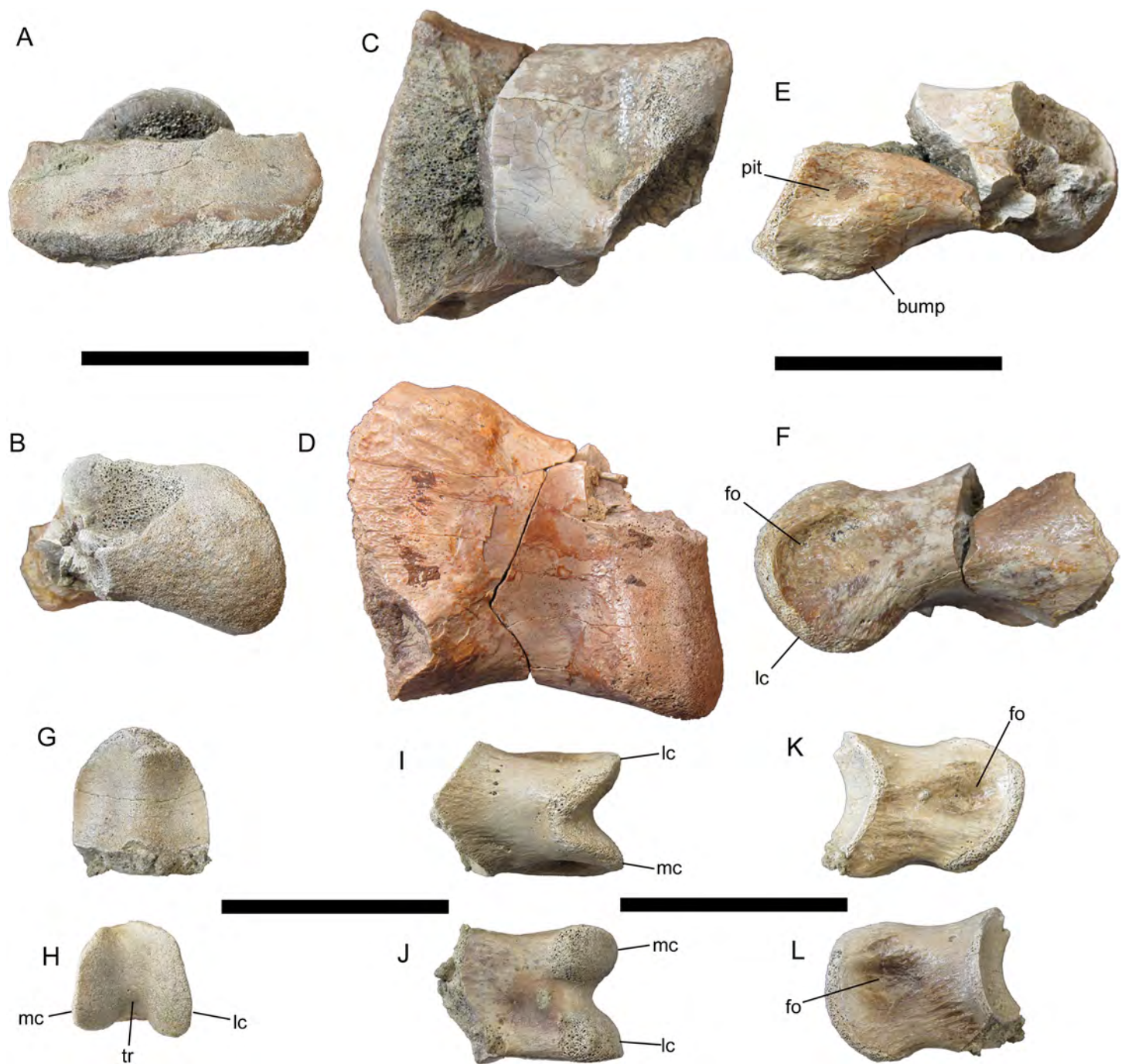


Figure 11 Pedal phalanges of UMNH VP 28348. Phalanx 2 of left pedal digit IV in (A) proximal; (B) distal; (C) dorsal; (D) ventral; (E) medial; and (F) lateral views. Phalanx 4 of left pedal digit IV in (G) proximal; (H) distal; (I) dorsal; (J) ventral; (K) medial; and (L) lateral views. Abbreviations: fo, fovea; lc, lateral condyle; mc, medial condyle; tr, trochlea. Scale bars equal five cm. [Full-size !\[\]\(bea84fde67c72a6490eeb6cd10f75669_img.jpg\) DOI: 10.7717/peerj.5749/fig-11](https://doi.org/10.7717/peerj.5749/fig-11)

DISCUSSION

Tyrannosaurid phylogeny

The topology of the strict consensus cladogram (Fig. 12) is identical to that of Carr *et al.* (2017), except for a lack of resolution among large-bodied derived tyrannosaurines,

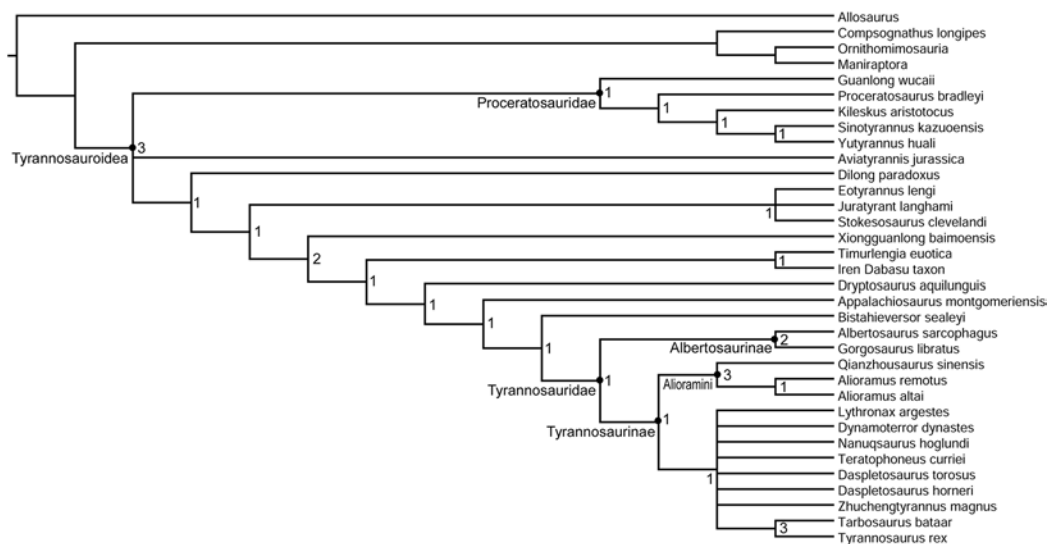


Figure 12 Phylogenetic relationships of *Dynamoterror dynastes*. Strict consensus cladogram of 18 most parsimonious trees obtained by TNT. Tree image was prepared in Mesquite. Bremer support values are next to each node. [Full-size !\[\]\(78455399e1afe561232b644638671568_img.jpg\) DOI: 10.7717/peerj.5749/fig-12](https://doi.org/10.7717/peerj.5749/fig-12)

including *Dynamoterror*, *Teratophoneus*, *Lythronax*, *Nanuqsaurus*, *Daspletosaurus*, *Zhuchengtyrannus*, and a clade composed of *Tarbosaurus* and *Tyrannosaurus*. This is probably due to the inclusion of the fragmentary new taxon *Dynamoterror*. Determining an area of origin for this large-bodied tyrannosaurine clade is difficult due to the paucity of the tyrannosauroid record from the Campanian of Asia ([Brusatte & Carr, 2016](#)) and the lack of diagnostic early tyrannosaurids from northern Laramidia. Two tyrannosaurids are now known from the lower Campanian of southern Laramidia, *L. argestes* from the Wahweap Formation of Utah ([Loewen et al., 2013](#)) and *Dynamoterror dynastes* from the Allison Member of the Menefee Formation of New Mexico. However, diagnostic tyrannosaurid material is currently lacking from roughly contemporaneous units in northern Laramidia, such as the lower Two Medicine Formation and McClelland Ferry Member of the Judith River Formation of Montana, and the Deadhorse Coulee Member of the Milk River Formation, Foremost Formation, and lower Oldman Formation of Alberta ([Fowler, 2017](#)). Furthermore, the early evolution and biogeography of Tyrannosaurinae in southern Laramidia remain enigmatic pending the discovery of additional tyrannosaurine material from the Menefee, Wahweap, and Kaiparowits formations. The current paucity of tyrannosauroid material from Santonian and lower Campanian units in Laramidia also hampers comparison with the tyrannosauroid record from Appalachia ([Schwimmer et al., 1993, 2015](#); [Carr, Williamson & Schwimmer, 2005](#); [Brusatte, Benson & Norell, 2011](#); [Brownstein, 2017](#); [Dalman, Jasinski & Lucas, 2017](#)).

Reconstructing *Dynamoterror dynastes*

The dimensions of the frontals of UMNH VP 28348 are similar to those of LACM 23845, a subadult specimen of *Tyrannosaurus rex* ([Currie, 2003](#); [Carr & Williamson, 2004](#)), suggesting roughly similar skull and body size, with the caveat that the proportions of

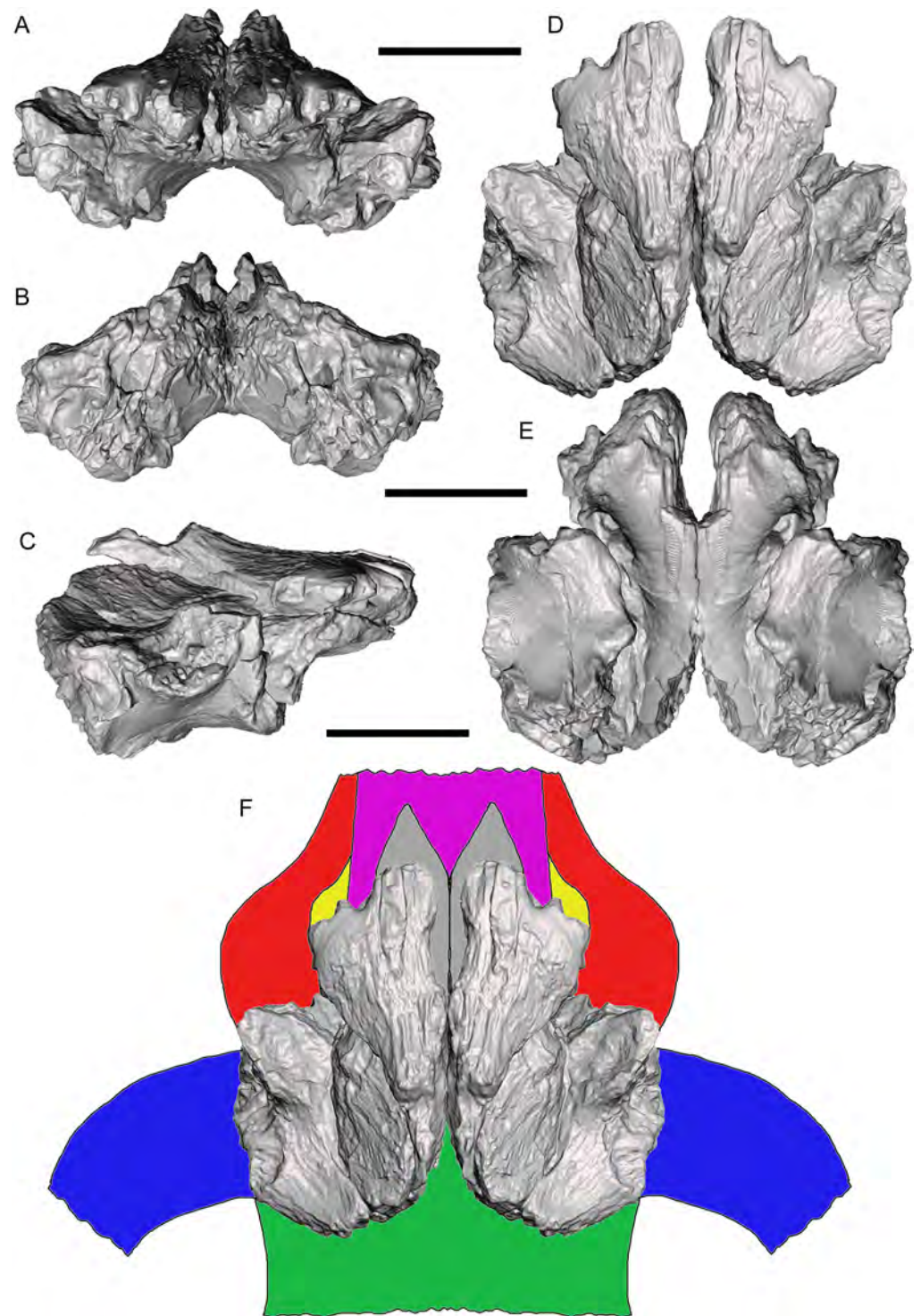


Figure 13 Reconstructed frontal complex of *Dynamoterror dynastes*. Composite, articulated right and left frontals in (A) rostral; (B) caudal; (C) right lateral; (D) dorsal; and (E) ventral views. (F) Reconstructed skull roof in dorsal view. Elements are color-coded as follows: frontals (gray); fused nasals (violet); prefrontals (yellow); lacrimals (red); postorbitals (blue); and parietal (green). Missing elements reconstructed based upon *Teratophoneus curriei* (UMNH VP 16690) (Loewen et al., 2013). Scale bars equal five cm. [Full-size !\[\]\(2154c9f569edab9d15ee6b3ae0aa8398_img.jpg\) DOI: 10.7717/peerj.5749/fig-13](https://doi.org/10.7717/peerj.5749/fig-13)

these two individuals might have been different depending upon their relative ontogenetic stages. According to [Molnar \(1980\)](#), LACM 23845 is approximately 80% the size of an adult *Tyrannosaurus rex*. If UMNH VP 28348 was of similar size to LACM 23845, then this subadult or adult individual of *Dynamoterror dynastes* was about 30 feet long, a medium-sized tyrannosaurid.

Three-dimensional digital models of the described elements of UMNH VP 28348 were created by laser-scanning the bones. These models are available at MorphoSource under the project name “A new tyrannosaurid from the Upper Cretaceous Menefee Formation of New Mexico.” The models of the right and left frontals were aligned and combined on the basis of overlapping features, creating a composite pair that is nearly complete except for the nasal processes ([Figs. 13A–13E](#)). This allowed the frontal region of the skull roof to be reconstructed with some confidence based upon the positions, sizes, and morphologies of the nasal, prefrontal, lacrimal, postorbital, and parietal contacts ([Fig. 13F](#)). Several salient tyrannosaurine features can be observed on the reconstructed skull roof of *Dynamoterror*, such as large supratemporal fossae and a tall sagittal crest on the frontals, providing an expanded attachment area for enormous jaw-closing muscles ([Currie, 2003](#); [Carr & Williamson, 2004](#); [Holliday, 2009](#)).

CONCLUSIONS

The description of *Dynamoterror dynastes* from the lower Campanian Allison Member of the Menefee Formation provides additional data on the morphology and diversity of early tyrannosaurines in Laramidia. However, additional discoveries are needed to elucidate the paleobiogeographic history of tyrannosaurines.

INSTITUTIONAL ABBREVIATIONS

BYU Brigham Young University Museum of Paleontology, Provo, Utah, USA
LACM Natural History Museum of Los Angeles County, Los Angeles, California, USA
UMNH Natural History Museum of Utah (formerly Utah Museum of Natural History), Salt Lake City, Utah, USA.

ACKNOWLEDGEMENTS

We are grateful to Hazel and Christopher Wolfe of the Zuni Dinosaur Institute for Geosciences for their ongoing support in every phase of this project. UMNH VP 28348 was found in August 2012 by Eric Gutierrez and collected by Sam Cordero, W. H. and Nancy Ebbinghaus, Eric Gutierrez, Brandon Hedrick, Jake Kudlinski, Adam Laing, Andrew T. McDonald, Sherman and Ben Mohler, James Poole, John Rockhill, Korri Dee Turner, Brian Watkins, and Douglas G. Wolfe. We thank UMNH staff (Tylor Birthisel, Randall Irmis, Janaki Krishna, Carolyn Levitt-Bussian, and Megan Mizuta) for curation and loan of UMNH VP 28348 to Western Science Center (WSC). Brett Dooley (WSC) scanned UMNH VP 28348. We are grateful to Brett Dooley and Brittney Stoneburg (WSC) for discussions about the tyrant dinosaurs. ATM thanks Rod Scheetz (BYU) for photos of *Teratophoneus curriei* frontal BYU 8120/9396 and permission to use them, and other colleagues for access to tyrannosaurid specimens under their care

(Maureen Walsh, LACM; and Randall Irmis and Carolyn Levitt-Bussian, UMNH). The Willi Hennig Society is acknowledged for making TNT freely usable. We thank the Academic Editor, John Hutchinson, and the reviewers, Chase Brownstein, Stephen Brusatte, and Thomas D. Carr, for reviews that improved the paper.

ADDITIONAL INFORMATION AND DECLARATIONS

Funding

The field work that led to discovery of the specimen was supported by grants from the Western Interior Paleontological Society, Geological Society of America, and University of Pennsylvania. The funders had no role in study design, data collection and analysis, decision to publish, or preparation of the manuscript.

Grant Disclosures

The following grant information was disclosed by the authors:

Western Interior Paleontological Society, Geological Society of America, and University of Pennsylvania.

Competing Interests

The authors declare that they have no competing interests. Andrew T. McDonald and Alton C. Dooley Jr. are employed by Western Science Center, Hemet, California, and Douglas G. Wolfe is employed by Zuni Dinosaur Institute for Geosciences, Springerville, Arizona.

Author Contributions

- Andrew T. McDonald conceived and designed the experiments, performed the experiments, analyzed the data, contributed reagents/materials/analysis tools, prepared figures and/or tables, authored or reviewed drafts of the paper, approved the final draft.
- Douglas G. Wolfe conceived and designed the experiments, performed the experiments, analyzed the data, contributed reagents/materials/analysis tools, authored or reviewed drafts of the paper, approved the final draft.
- Alton C. Dooley Jr conceived and designed the experiments, performed the experiments, analyzed the data, contributed reagents/materials/analysis tools, prepared figures and/or tables, authored or reviewed drafts of the paper, approved the final draft.

Field Study Permissions

The following information was supplied relating to field study approvals (i.e., approving body and any reference numbers):

The specimen described herein was collected under permit NM12-03S issued by the U.S. Bureau of Land Management.

Data Availability

The following information was supplied regarding data availability:

The supplemental file includes a list of phylogenetic characters coded for the new taxon and a table of measurements of the fossil specimen.

New Species Registration

The following information was supplied regarding the registration of a newly described species:

Publication LSID: urn:lsid:zoobank.org:pub:E6547114-4285-49BB-AF82-1280F631748F

Dynamoterror LSID: urn:lsid:zoobank.org:act:4B3FA975-DC43-4C1F-813F-29BB9DFDF9B6,

Dynamoterror dynastes LSID: urn:lsid:zoobank.org:act:EED48535-DC9C-4E4A-A5BB-1ACA1D5FD918.

Supplemental Information

Supplemental information for this article can be found online at <http://dx.doi.org/10.7717/peerj.5749#supplemental-information>.

REFERENCES

- Baron MG, Norman DB, Barrett PM. 2017.** A new hypothesis of dinosaur relationships and early dinosaur evolution. *Nature* **543(7646)**:501–506 DOI [10.1038/nature21700](https://doi.org/10.1038/nature21700).
- Bever GS, Brusatte SL, Carr TD, Xu X, Balanoff AM, Norell MA. 2013.** The braincase anatomy of the Late Cretaceous dinosaur *Alioramus* (Theropoda: Tyrannosauroida). *Bulletin of the American Museum of Natural History* **376(1)**:1–72 DOI [10.1206/810.1](https://doi.org/10.1206/810.1).
- Brochu CA. 2003.** Osteology of *Tyrannosaurus rex*: insights from a nearly complete skeleton and high-resolution computed tomographic analysis of the skull. *Journal of Vertebrate Paleontology* **22(4)**:1–138 DOI [10.2307/3889334](https://doi.org/10.2307/3889334).
- Brownstein CD. 2017.** A tyrannosauroid metatarsus from the Merchantville Formation of Delaware increases the diversity of non-tyrannosaurid tyrannosauroids on Appalachia. *PeerJ* **5**:e4123 DOI [10.7717/peerj.4123](https://doi.org/10.7717/peerj.4123).
- Brusatte SL, Benson RBJ, Norell MA. 2011.** The anatomy of *Dryptosaurus aquilunguis* (Dinosauria: Theropoda) and a review of its tyrannosauroid affinities. *American Museum Novitates* **3717(3717)**:1–53 DOI [10.1206/3717.2](https://doi.org/10.1206/3717.2).
- Brusatte SL, Carr TD. 2016.** The phylogeny and evolutionary history of tyrannosauroid dinosaurs. *Scientific Reports* **6(1)**:20252 DOI [10.1038/srep20252](https://doi.org/10.1038/srep20252).
- Brusatte SL, Carr TD, Erickson GM, Bever GS, Norell MA. 2009.** A long-snouted, multihorned tyrannosaurid from the Late Cretaceous of Mongolia. *Proceedings of the National Academy of Sciences of the United States of America* **106(41)**:17261–17266 DOI [10.1073/pnas.0906911106](https://doi.org/10.1073/pnas.0906911106).
- Carr TD. 2010.** A taxonomic assessment of the type series of *Albertosaurus sarcophagus* and the identity of Tyrannosauridae (Dinosauria, Coelurosauria) in the *Albertosaurus* bonebed from the Horseshoe Canyon Formation (Campanian–Maastrichtian, Late Cretaceous). *Canadian Journal of Earth Sciences* **47(9)**:1213–1226 DOI [10.1139/e10-035](https://doi.org/10.1139/e10-035).
- Carr TD, Varricchio DJ, Sedlmayr JC, Roberts EM, Moore JR. 2017.** A new tyrannosaur with evidence for anagenesis and crocodile-like facial sensory system. *Scientific Reports* **7(1)**:44942 DOI [10.1038/srep44942](https://doi.org/10.1038/srep44942).
- Carr TD, Williamson TE. 2000.** A review of Tyrannosauridae (Dinosauria, Coelurosauria) from New Mexico. In: Lucas SG, Heckert AB, eds. *Dinosaurs of New Mexico*. Vol. 17. Albuquerque: New Mexico Museum of Natural History and Science Bulletin, 113–145.
- Carr TD, Williamson TE. 2004.** Diversity of late Maastrichtian Tyrannosauridae (Dinosauria: Theropoda) from western North America. *Zoological Journal of the Linnean Society* **142(4)**:479–523 DOI [10.1111/j.1096-3642.2004.00130.x](https://doi.org/10.1111/j.1096-3642.2004.00130.x).

- Carr TD, Williamson TE. 2010.** *Bistahieversor sealeyi*, gen. et sp. nov., a new tyrannosauroid from New Mexico and the origin of deep snouts in Tyrannosauroidea. *Journal of Vertebrate Paleontology* **30**(1):1–16 DOI [10.1080/02724630903413032](https://doi.org/10.1080/02724630903413032).
- Carr TD, Williamson TE, Britt BB, Stadtman K. 2011.** Evidence for high taxonomic and morphologic tyrannosauroid diversity in the Late Cretaceous (late Campanian) of the American Southwest and a new short-skulled tyrannosaurid from the Kaiparowits Formation of Utah. *Naturwissenschaften* **98**(3):241–246 DOI [10.1007/s00114-011-0762-7](https://doi.org/10.1007/s00114-011-0762-7).
- Carr TD, Williamson TE, Schwimmer DR. 2005.** A new genus and species of tyrannosauroid from the Late Cretaceous (middle Campanian) Demopolis Formation of Alabama. *Journal of Vertebrate Paleontology* **25**(1):119–143 DOI [10.1671/0272-4634\(2005\)025\[0119:angaso\]2.0.co;2](https://doi.org/10.1671/0272-4634(2005)025[0119:angaso]2.0.co;2).
- Cohen KM, Finney SC, Gibbard PL, Fan J-X. 2013.** The ICS International Chronostratigraphic Chart. *Episodes* **36**:199–204.
- Currie PJ. 2003.** Cranial anatomy of tyrannosaurid dinosaurs from the Late Cretaceous of Alberta, Canada. *Acta Palaeontologica Polonica* **48**:191–226.
- Dalman SG, Jasinski SE, Lucas SG. 2017.** First occurrence of a tyrannosauroid dinosaur from the lower Campanian Merchantville Formation of Delaware, USA. *Memoirs of the Fukui Prefectural Museum* **16**:29–38.
- Fiorillo AR, Tykoski RS. 2014.** A diminutive new tyrannosaur from the top of the world. *PLOS ONE* **9**(3):e91287 DOI [10.1371/journal.pone.0091287](https://doi.org/10.1371/journal.pone.0091287).
- Fowler DW. 2017.** Revised geochronology, correlation, and dinosaur stratigraphic ranges of the Santonian-Maastrichtian (Late Cretaceous) formations of the Western Interior of North America. *PLOS ONE* **12**(11):e0188426 DOI [10.1371/journal.pone.0188426](https://doi.org/10.1371/journal.pone.0188426).
- Goloboff PA, Catalano SA. 2016.** TNT version 1.5, including a full implementation of phylogenetic morphometrics. *Cladistics* **32**(3):221–238 DOI [10.1111/cla.12160](https://doi.org/10.1111/cla.12160).
- Holliday CM. 2009.** New insights into dinosaur jaw muscle anatomy. *Anatomical Record* **292**(9):1246–1265 DOI [10.1002/ar.20982](https://doi.org/10.1002/ar.20982).
- Holtz TR Jr. 2004.** Tyrannosauroidea. In: Weishampel DB, Dodson P, Osmólska H, eds. *The Dinosauria*. Berkeley: University of California Press, 111–136.
- Hone DWE, Wang K, Sullivan C, Zhao X, Chen S, Li D, Ji S, Ji Q, Xu X. 2011.** A new, large tyrannosaurine theropod from the Upper Cretaceous of China. *Cretaceous Research* **32**(4):495–503 DOI [10.1016/j.cretres.2011.03.005](https://doi.org/10.1016/j.cretres.2011.03.005).
- Huene FV. 1914.** Beiträge zur geschichte der Archosaurier (contribution to the history of the archosaurs). *Geologie und Paläontologie Abhandlungen* **13**(7):1–56.
- Hunt AP, Lucas SG. 1993.** Cretaceous vertebrates of New Mexico. In: Lucas SG, Zidek J, eds. *Vertebrate Paleontology in New Mexico*. Vol. 2. Albuquerque: New Mexico Museum of Natural History and Science Bulletin, 77–91.
- Hurum JH, Sabath K. 2003.** Giant theropod dinosaurs from Asia and North America: skulls of *Tarbosaurus bataar* and *Tyrannosaurus rex* compared. *Acta Palaeontologica Polonica* **48**:161–190.
- Kurzanov SM. 1976.** A new Late Cretaceous carnosaur from Nogon-Tsav Mongolia. *Sovmestnaâ Sovetsko-Mongolskaâ Paleontologiceskaâ Ekspeditciâ, Trudy* **3**:93–104 [in Russian].
- Larson P. 2008.** Atlas of the skull bones of *Tyrannosaurus rex*. In: Larson P, Carpenter K, eds. *Tyrannosaurus rex: The Tyrant King*. Bloomington: Indiana University Press, 233–243.
- Lehman TM, Carpenter K. 1990.** A partial skeleton of the tyrannosaurid dinosaur *Aublysodon* from the Upper Cretaceous of New Mexico. *Journal of Paleontology* **64**(6):1026–1032 DOI [10.1017/s0022336000019843](https://doi.org/10.1017/s0022336000019843).

- Lehman TM, Wick SL. 2012.** Tyrannosauroid dinosaurs from the Aguja Formation (Upper Cretaceous) of Big Bend National Park, Texas. *Earth and Environmental Science Transactions of the Royal Society of Edinburgh* **103(3–4)**:471–485
DOI [10.1017/s1755691013000261](https://doi.org/10.1017/s1755691013000261).
- Lewis C. 2006.** A microvertebrate fauna of the Upper Cretaceous (late Santonian-early Campanian) Menefee Formation, northwestern New Mexico. *Geological Society of America Abstracts with Programs* **38**:69.
- Loewen MA, Irmis RB, Sertich JJW, Currie PJ, Sampson SD. 2013.** Tyrant dinosaur evolution tracks the rise and fall of Late Cretaceous oceans. *PLOS ONE* **8(11)**:e79420
DOI [10.1371/journal.pone.0079420](https://doi.org/10.1371/journal.pone.0079420).
- Lü J, Yi L, Brusatte SL, Yang L, Li H, Chen L. 2014.** A new clade of Asian Late Cretaceous long-snouted tyrannosaurids. *Nature Communications* **5(1)**:3788 DOI [10.1038/ncomms4788](https://doi.org/10.1038/ncomms4788).
- Lucas SG, Spielmann JA, Braman DR, Brister BS, Peters L, McIntosh WC. 2005.** Age of the Cretaceous Menefee Formation, Gallina hogback, Rio Arriba County, New Mexico. In: Lucas SG, Zeigler KE, Lueth VW, Owen DE, eds. *New Mexico Geological Society 56th Annual Fall Field Conference Guidebook*. Socorro: Geology of the Chama Basin, 231–235.
- Marsh OC. 1881.** Classification of the Dinosauria. *American Journal of Science* **s3-23(133)**:81–86
DOI [10.2475/ajs.s3-23.133.81](https://doi.org/10.2475/ajs.s3-23.133.81).
- Matthew WD, Brown B. 1922.** The family Deinodontidae, with notice of a new genus from the Cretaceous of Alberta. *Bulletin of the American Museum of Natural History* **46**:367–385.
- Miller RL, Carey MA, Thompson-Rizer CL. 1991.** *Geology of the La Vida Mission Quadrangle, San Juan and McKinley Counties, New Mexico*. Vol. 1940. Denver: U.S. Geological Survey Bulletin, 1–64.
- Molenaar CM, Cobban WA, Merewether EA, Pillmore CL, Wolfe DG, Holbrook JM. 2002.** *Regional Stratigraphic Cross Sections of Cretaceous Rocks from East-Central Arizona to the Oklahoma Panhandle*. Denver: U.S. Geological Survey Miscellaneous Field Studies Map MF-2382.
- Molnar RE. 1974.** A distinctive theropod dinosaur from the Upper Cretaceous of Baja California (Mexico). *Journal of Paleontology* **48**:1009–1017.
- Molnar RE. 1980.** An albertosaur from the Hell Creek Formation of Montana. *Journal of Paleontology* **54**:102–108.
- Osborn HF. 1905.** *Tyrannosaurus* and other Cretaceous carnivorous dinosaurs. *Bulletin of the American Museum of Natural History* **21**:259–265.
- Osborn HF. 1906.** *Tyrannosaurus*, Upper Cretaceous carnivorous dinosaur (Second communication). *Bulletin of the American Museum of Natural History* **22**:281–296.
- Osborn HF. 1912.** Crania of *Tyrannosaurus* and *Allosaurus*. *Memoirs of the American Museum of Natural History* **1**:1–30.
- Owen R. 1842.** Report on British fossil reptiles, part II. *Reports of the British Association for the Advancement of Sciences* **11**:60–204.
- Renne PR, Deino AL, Hilgen FJ, Kuiper KF, Mark DF, Mitchell WS III, Morgan LE, Mundil R, Smit J. 2013.** Time scales of critical events around the Cretaceous-Paleogene boundary. *Science* **339(6120)**:684–687 DOI [10.1126/science.1230492](https://doi.org/10.1126/science.1230492).
- Russell DA. 1970.** Tyrannosaurs from the Late Cretaceous of western Canada. *National Museum of Natural Sciences Publications in Paleontology* **1**:1–34.
- Sampson SD, Loewen MA. 2005.** *Tyrannosaurus rex* from the Upper Cretaceous (Maastrichtian) North Horn Formation of Utah: biogeographic and paleoecologic implications. *Journal of Vertebrate Paleontology* **25(2)**:469–472 DOI [10.1671/0272-4634\(2005\)025\[0469:trftuc\]2.0.co;2](https://doi.org/10.1671/0272-4634(2005)025[0469:trftuc]2.0.co;2).

- Sampson SD, Loewen MA, Farke AA, Roberts EM, Forster CA, Smith JA, Titus AL. 2010.** New horned dinosaurs from Utah provide evidence for intracontinental dinosaur endemism. *PLOS ONE* 5(9):e12292 DOI [10.1371/journal.pone.0012292](https://doi.org/10.1371/journal.pone.0012292).
- Schwimmer DR, Sanders AE, Erickson BR, Weems RE. 2015.** A Late Cretaceous dinosaur and reptile assemblage from South Carolina, USA. *Transactions of the American Philosophical Society* 105:1–157.
- Schwimmer DR, Williams GD, Dobie JL, Siesser WG. 1993.** Late Cretaceous dinosaurs from the Blufftown Formation in western Georgia and eastern Alabama. *Journal of Paleontology* 67(2):288–296 DOI [10.1017/s0022336000032212](https://doi.org/10.1017/s0022336000032212).
- Sereno PC, McAllister S, Brusatte SL. 2005.** TaxonSearch: a relational database for suprageneric taxa and phylogenetic definitions. *PhyloInformatics* 8:1–21.
- Siemers CT, King NR. 1974.** Macroinvertebrate paleoecology of a transgressive marine sandstone, Cliff House Sandstone (Upper Cretaceous), Chaco Canyon, northwestern New Mexico. In: *New Mexico Geological Society Guidebook, 25th Field Conference*. Ghost Ranch (Central-Northern N.M.), 267–277.
- Tsuihiji T, Watabe M, Tsogtbaatar K, Tsubamoto T, Barsbold R, Suzuki S, Lee AH, Ridgely RC, Kawahara Y, Witmer LM. 2011.** Cranial osteology of a juvenile specimen of *Tarbosaurus bataar* (Theropoda, Tyrannosauridae) from the Nemegt Formation (Upper Cretaceous) of Bugin Tsav, Mongolia. *Journal of Vertebrate Paleontology* 31(3):497–517 DOI [10.1080/02724634.2011.557116](https://doi.org/10.1080/02724634.2011.557116).
- Walker AD. 1964.** Triassic reptiles from the Elgin area: *Ornithosuchus* and the origin of carnosaurs. *Philosophical Transactions of the Royal Society B: Biological Sciences* 248(744):53–134 DOI [10.1098/rstb.1964.0009](https://doi.org/10.1098/rstb.1964.0009).
- Witmer LM, Ridgely RC. 2009.** New insights into the brain, braincase, and ear region of tyrannosaurs (Dinosauria, Theropoda), with implications for sensory organization and behavior. *Anatomical Record: Advances in Integrative Anatomy and Evolutionary Biology* 292(9):1266–1296 DOI [10.1002/ar.20983](https://doi.org/10.1002/ar.20983).